2022-07

Acute bioenergetic insulin sensitivity of skeletal muscle cells: ATP-demand-provoked glycolysis contributes to stimulation of ATP supply

Donnell, RA

http://hdl.handle.net/10026.1/19240

Contents lists available at ScienceDirect

Biochemistry and Biophysics Reports

Acute bioenergetic insulin sensitivity of skeletal muscle cells: ATP-demand-provoked glycolysis contributes to stimulation of ATP supply

Rosie A. Donnell, Jane E. Carré, Charles Affourtit [*]

School of Biomedical Sciences, University of Plymouth, John Bull Building, Plymouth Science Park, 16 Research Way, PL6 8BU, Plymouth, UK

A B S T R A C T

Skeletal muscle takes up glucose in an insulin-sensitive manner and is thus important for the maintenance of blood glucose homeostasis. Insulin resistance during development of type 2 diabetes is associated with decreased ATP synthesis, but the causality of this association is controversial. In this paper, we report real-time oxygen uptake and medium acidification data that we use to quantify acute insulin effects on intracellular ATP supply and ATP demand in rat and human skeletal muscle cells. We demonstrate that insulin increases overall cellular ATP supply by stimulating the rate of glycolytic ATP synthesis. Stimulation is immediate and achieved directly by increased glycolytic capacity, and indirectly by elevated ATP demand from protein synthesis. Raised glycolytic capacity does not result from augmented glucose uptake. Notably, insulin-sensitive glucose uptake is increased synergistically by nitrite. While nitrite has a similar stimulatory effect on glycolytic ATP supply as insulin, it does not amplify insulin stimulation. These data highlight the multifarious nature of acute bioenergetic insulin sensitivity of skeletal muscle cells, and are thus important for the interpretation of changes in energy metabolism that are seen in insulin-resistant muscle.

1. Introduction

Skeletal muscle is crucial for maintaining physiological glucose homeostasis, as it accounts for more than 70% of postprandial glucose disposal [1]. Muscle glucose uptake is stimulated by insulin [2], an anabolic hormone secreted by pancreatic beta cells when the blood glucose concentration increases after a meal [3]. Defects in glucose-stimulated insulin secretion and muscle insulin sensitivity, which often arise in obesity [4], both contribute to the development of type 2 diabetes [2]. Pathological mechanisms remain to be unravelled fully, but circulating nutrient excess and pro-inflammatory cytokines are widely recognised risk factors for muscle [5] and beta cell [6] dysfunction. Insulin resistance also manifests itself during loss of skeletal muscle function and mass (sarcopenia – [7]) that is associated with ageing [8] and chronic medical disorders such as advanced liver disease [9] and chronic kidney disease [10].

The insulin sensitivity of skeletal muscle benefits from energy demand induced by physical effort. Muscle cells take up glucose independently of insulin during exercise, but expression of insulin-sensitive glucose transporters is increased immediately after exercise [11]. This exercise benefit is mimicked by pharmacological stimulation of

AMP-activated protein kinase [11], the 'master regulator' of energy metabolism that is triggered physiologically when ATP demand is high [12]. Notably, glucose uptake during exercise may involve nitric oxide [13], which is generated during the oxidation of ʟ-arginine by nitric oxide synthases [14], but can also be made by reducing inorganic nitrate obtained from food [15]. Dietary nitrate has been shown to increase insulin sensitivity in rodent models, and has thus been suggested to protect against metabolic disease [15].

Insulin regulates muscle metabolism through an extensive network of signalling pathways [5] that are inhibited during development of metabolic disease by molecules that accumulate when nutrient supply persistently outweighs energy demand [16]. Reactive oxygen species are examples of such molecules [17], indicating causal involvement of mitochondrial redox biology in insulin resistance. Decreased mitochondrial ATP synthesis is associated strongly with insulin resistance too, but the causality of this bioenergetic association is less clear [16]. Insulin stimulates anabolism [5], and is thus expected to raise energy demand. Consistently, hyperinsulinemic euglycemic clamps increase mitochondrial ATP synthesis in human muscle [18–20] and, more acutely, insulin increases coupling efficiency [21] and ADP sensitivity [22] of oxidative phosphorylation in cultured muscle cells.

Following the appearance of convenient methods for quantifying

* Corresponding author.
E-mail address: charles.affourtit@plymouth.ac.uk (C. Affourtit).

Abbreviations

2DG	2-deoxyglucose
BAM15	N5,N6-bis(2-fluorophenyl)[1,2,5]oxadiazolo[3,4-b]pyrazine-5,6-diamine
DMEM	Dulbecco's modified Eagle medium
ECAR	extracellular acidification rate
FBS	fetal bovine serum
KRH	Hepes-buffered Krebs-Ringer medium
OCR	oxygen consumption rate
XF	extracellular flux

intracellular ATP production and consumption rates [23], we set out to further explore the bioenergetic insulin sensitivity of skeletal muscle cells. Here we show that insulin acutely stimulates the rate of overall ATP synthesis in clonal rat and primary human myocytes by increasing glycolytic ATP supply. In part, increased glycolysis is an adaptive response to insulin-provoked energy demand from protein synthesis.

2. Materials and methods

2.1. Tissue culture

Clonal rat myoblasts (L6.C11) were obtained from the European Collection of Cell Culture. L6 myoblasts were cultured at 37 °C under a humidified carbogen atmosphere of 5% CO_2 and 95% air in Dulbecco's modified Eagle medium (DMEM) that contained 5 mM glucose, 4 mM glutamine and 2 mM sodium pyruvate, and that was supplemented with 10% (v/v) fetal bovine serum (FBS). To allow differentiation, myoblasts were grown to complete confluence in fully supplemented DMEM, at which point the FBS concentration was decreased to 2% (v/v). This medium was refreshed every 2 days for 8 days when almost all myoblasts had visibly turned into myotubes.

Primary human skeletal muscle cells (CC-2561) were purchased from Lonza Bioscience and treated exactly as prescribed by Lonza's detailed instructions for using their Clonetics™ cell systems (https://bioscience.lonza.com/lonza_bs/GB/en/download/product/asset/29428). The gestational tissue from which these human myoblasts were isolated, was donated by healthy individuals. To differentiate them to myotubes, myoblasts were grown to 50–60% confluence and were then incubated for 5 days in fusion medium (DMEM:F-12 – Sigma 12–719F) with 2% (v/v) horse serum (Sigma 14-403E), at which point cellular bioenergetics were analysed as described next.

2.2. Cellular bioenergetics

Oxygen uptake and medium acidification by intact L6 and human myocytes were measured simultaneously, with Seahorse XF24 and XFe96 analysers (Agilent), respectively. Before the assay, cells were washed into a Hepes-buffered Krebs-Ringer medium (KRH) comprising 135 mM NaCl, 3.6 mM KCl, 2 mM Hepes (pH 7.4), 0.5 mM $MgCl_2$, 1.5 mM $CaCl_2$, 0.5 mM NaH_2PO_4 and 5 mM glucose. Cells were incubated in KRH for 90 min under air at 37 °C, and then transferred to the analyser for equilibration. As specified in the Figure legends, 100 nM human insulin (Sigma I9278-5 ML) was added immediately before this equilibration, and/or cells were transiently exposed to 1 μM $NaNO_2$ for the final 20 min of the 90-min pre-incubation. The basal oxygen consumption (OCR) and extracellular acidification (ECAR) rates were recorded, after which oligomycin, N5,N6-bis(2-fluorophenyl)[1,2,5]oxadiazolo-[3,4-b]pyrazine-5,6-diamine (BAM15) and rotenone/antimycin A were added sequentially to inhibit the ATP synthase, uncouple oxidative phosphorylation, and inhibit the mitochondrial electron transfer chain, respectively. Effector concentrations are given for L6 and human cells in

Figs. 1 and 3, respectively. The OCR was calculated from time-resolved oxygen concentrations applying the *Akos* algorithm [24]. OCR and ECAR were normalised to protein content determined by the bicinchoninic acid assay [25].

Glycolytic and oxidative ATP supply rates were calculated from cellular oxygen uptake and medium acidification as described in full detail by others [23], assuming that cellular energy metabolism was fuelled exclusively by glucose. This assumption is reasonable on the whole, because glucose is the sole carbon fuel in the KRH we used, but glycolytic ATP supply rates may be somewhat underestimated in runs without glucose when myocytes likely break down glycogen. The rate of mitochondrial ATP supply was calculated from ATP-synthesis-coupled respiration using P/O ratios for Krebs cycle turnover and oxidative phosphorylation of 0.12 and 2.5, respectively, thus assuming glycolytic reducing power is transferred to mitochondria by the malate-aspartate shuttle alone. ATP-synthesis-coupled respiration was approximated from the oligomycin-sensitive OCR after correcting for the small underestimation owing to oligomycin-induced hyperpolarisation of the mitochondrial inner membrane [23]. Glycolytic ATP supply was defined as the net ATP produced during glucose breakdown to pyruvate irrespective of the destiny of pyruvate. The glycolytic ATP supply rate was thus calculated from medium acidification to account for pyruvate reduced to lactate⁻ plus H^+ (ATP:lactate = 1:1) and from mitochondrial respiration to account for the pyruvate oxidised to bicarbonate (ATP:O_2 = 0.33:1). A KRH buffering power of 0.681 mpH x μM^{-1} H^+ was used to convert the ECAR to a proton production rate assuming an effective XF24 measurement volume of 22.7 μL [24] and an XFe96 volume that is four times smaller, i.e., 5.7 μL.

2.3. Lactate production

Lactate released by L6 myoblasts was measured enzymatically as described in Ref. [26]. Cells grown in fully supplemented DMEM were washed into KRH and were assayed immediately under air at 37 °C in KRH that contained 5 mM glucose with or without 100 nM human insulin. Supernatant was removed at various time points (see Fig. 2E), and stored at room temperature until assay. Lactate concentration was determined from the initial rate of NADH production in an assay mixture comprised of 0.5 M Tris/HCl (pH 9.8), 10 mM EDTA, 200 mM hydrazine, 2 mM NAD^+ and 20 U/mL lactate dehydrogenase. NADH was detected by fluorescence ($\lambda_{ex/em}$ = 340/460 nm) in a PHERAstar FS plate reader (BMG Labtech). Released lactate amounts were normalised to protein content.

2.4. Glucose uptake

Uptake of 2-deoxyglucose (2DG) by L6 myocytes was measured as described in Ref. [21]. Cells grown in 2% instead of 10% (v/v) FBS from 16 h before the experiment were incubated for 1 h at 37 °C in glucose-free DMEM, then washed into glucose-free KRH supplemented with 0.1% (w/v) bovine serum albumin (BSA), and incubated in this medium ± 1 μM $NaNO_2$ for 30 min at 37 °C. Cells were incubated for another 20 min at 37 °C in fresh glucose-free KRH ±100 nM insulin at which point 5 mM 2DG was added. Following another 20-min incubation at 37 °C, cells were washed with glucose-free KRH, lysed in 0.1 N NaOH (10 min agitated incubation at 65 °C and 50 min at 85 °C), and neutralised with 0.1 N HCl in triethanolamine (200 mM, pH 8). 2DG concentration was determined from resorufin production during 50-min incubation at 37 °C in an assay mixture comprising 50 mM triethanolamine (pH 8), 50 mM KCl, 15 U/ml glucose-6-phosphate dehydrogenase, 0.2 U/ml diaphorase, 0.1 mM $NADP^+$, 0.02% (w/v) BSA and 2 μM resazurin. Resorufin was detected by fluorescence ($\lambda_{ex/em}$ = 540/590 nm) in a PHERAstar FS plate reader (BMG Labtech).
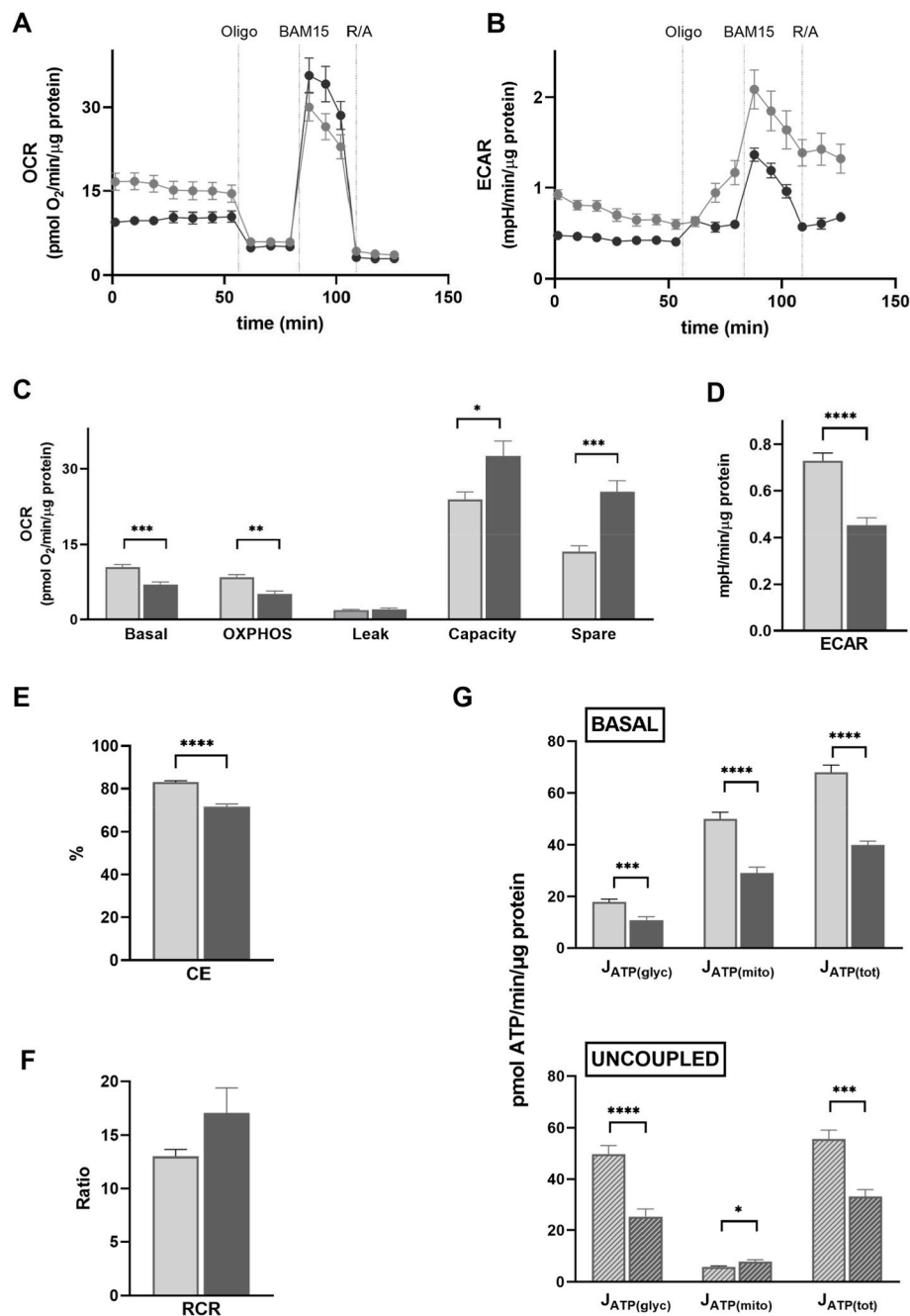
Fig. 1. – Bioenergetics of L6 myocytes. Myoblasts (light-grey symbols) and myotubes (dark-grey symbols) were grown and assayed in the presence of 5 mM glucose. Oxygen consumption rate (OCR) and extracellular acidification rate (ECAR) were measured in the absence and cumulative presence of 5 μg/mL oligomycin (Oligo), 0.7 μM N5,N6-bis(2-fluorophenyl)[1,2,5]oxadiazolo[3,4-b]pyrazine-5,6-diamine (BAM15), and 1 μM rotenone with 1 μM antimycin A (R/A). Mitochondrial OCRs (panel C), basal ECAR (panel D), coupling efficiency of oxidative phosphorylation (CE, panel E), and the cell respiratory control ratio (RCR, panel F) were derived as described in the text. Glycolytic, mitochondrial and total ATP supply ($J_{ATP(glyc)}$, $J_{ATP(mito)}$, $J_{ATP(tot)}$) rates were determined without effectors (BASAL, panel G) and in the presence of oligomycin and BAM15 (UNCOUPLED, panel G). Bioenergetic parameters reflecting the uncoupled state, were calculated from the peak OCR and ECAR values observed in the combined presence of oligomycin and BAM15. Data are means ± SEM of 6–34 separate measurements from 2 to 5 assays. Differences between myoblasts and myotubes were evaluated for statistical significance by Mann-Whitney tests (*$P < 0.05$, **$P < 0.01$, ***$P < 0.001$, ****$P < 0.0001$). Basal: mitochondrial OCR in the absence of effectors; OXPHOS: OCR coupled to ATP synthesis; Leak: OCR linked to mitochondrial proton leak; Capacity: mitochondrial OCR stimulated by BAM15; Spare: difference between Capacity and Basal.

2.5. Statistical analysis

Data are shown as means ± SEM. Differences between experimental groups were evaluated for statistical significance using GraphPad Prism software (version 9 for Windows) using tests specified in the figure legends.

3. Results and discussion

3.1. Quantification of ATP supply in skeletal muscle cells

Typical extracellular flux (XF) traces shown in Fig. 1A and B illustrate how the OCR and ECAR of L6 myocytes respond to mitochondrial effectors. The basal OCR decreases when mitochondrial ATP synthesis is inhibited with oligomycin. Dissipation of the protonmotive force with BAM15 then stimulates the OCR, more strongly in myotubes than

myoblasts, and inhibition of mitochondrial electron transfer with rotenone and antimycin A lowers it (Fig. 1A). The remaining OCR is subtracted from other OCRs to reveal mitochondrial respiratory rates (Fig. 1C). Myocytes compensate their inability to make ATP via oxidative phosphorylation in the presence of oligomycin/BAM15 by increasing the rate of anaerobic glycolysis, as is reflected by an increased ECAR (Fig. 1B).

The basal mitochondrial OCR (Fig. 1C) and basal ECAR (Fig. 1D) are lower in myotubes than in myoblasts. Respiration coupled to ATP synthesis (oligomycin-sensitive OCR) is also comparably low in myotubes, but respiration linked to mitochondrial proton leak (oligomycin-insensitive OCR) is the same (Fig. 1C). The percentage of basal mitochondrial respiration used to make ATP, i.e., coupling efficiency of oxidative phosphorylation [27], is thus higher in myoblasts than in myotubes (Fig. 1E). Respiratory capacity (BAM15-uncoupled OCR) is relatively high in myotubes (Fig. 1C), which explains the tendency to a higher cell
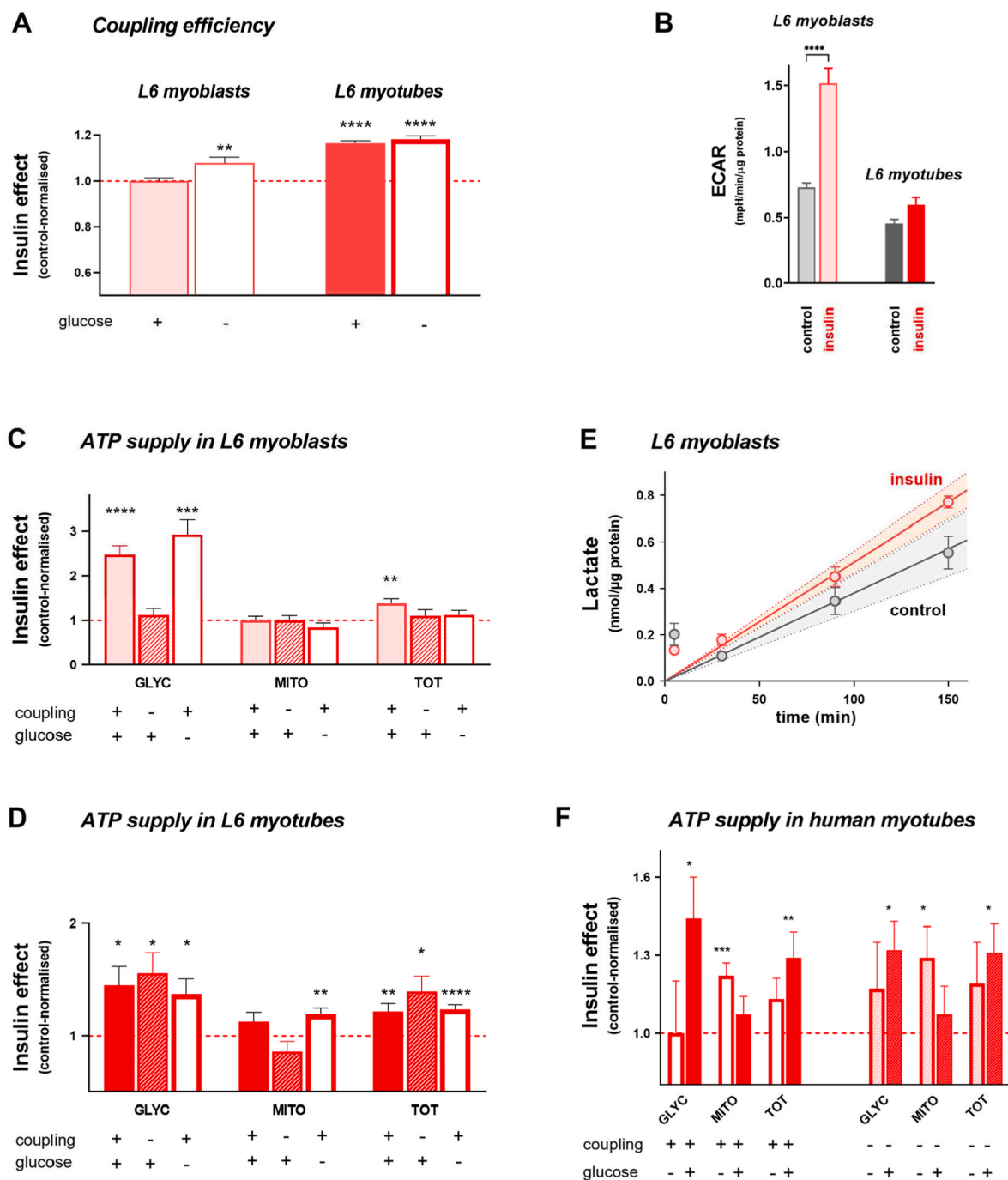
Fig. 2. – Insulin sensitivity of muscle cell bioenergetics. The acute effect of 100 nM human insulin on coupling efficiency of oxidative phosphorylation (panel A), ECAR (panel B), and on glycolytic (GLYC), mitochondrial (MITO) and total (TOT) ATP supply rates (panels C, D, F) was measured under basal (coupling +) and uncoupled (coupling –) conditions with or without 5 mM glucose. For glucose-free runs, myoblasts were cultured at 2% instead of 10% fetal bovine serum (FBS) from 16 h before the experiment. The insulin effects shown in panels A, C, D and F are expressed relative to the respective control parameters measured in the absence of insulin (cf. Fig. 1). Data are means ± SEM of 6–22 separate measurements from 2 to 4 independent XF runs. Absolute differences in panel B were evaluated for statistical significance by Mann-Whitney tests. Control-normalised effects were assessed for significance by one sample t tests (*P < 0.05, **P < 0.01, ***P < 0.001, ****P < 0.0001). Lactate release data from cells grown and assayed in the presence of 5 mM glucose (panel E), and assayed with and without 100 nM human insulin, are means ± SEM of 8–21 separate measurements from 2 to 5 independent assays, and were fitted to linear expressions 'forced' through the origin. The mean (SEM) fit slopes are 3.8 (0.39) and 5.1 (0.24) pmol lactate released per min per µg protein for control and insulin-exposed L6 myoblasts, respectively. The shaded areas between dotted lines reflect 95% confidence intervals.

respiratory control ratio (Fig. 1F), i.e., the ratio between BAM15-uncoupled and oligomycin-insensitive respiration [27]. Spare respiratory capacity (uncoupled OCR minus basal OCR) is 1.9-fold higher in myotubes than myoblasts (Fig. 1C). Glycolytic, mitochondrial and total ATP supply rates are lower in myotubes than myoblasts

under basal conditions (Fig. 1G). Mitochondrial ATP supply is relatively low under uncoupled conditions in both cell systems (Fig. 1G), because oligomycin and BAM15 prevent oxidative phosphorylation. Mitochondrial ATP supply is not abolished fully, however, as mitochondrial substrate-level phosphorylation increases when the respiratory chain
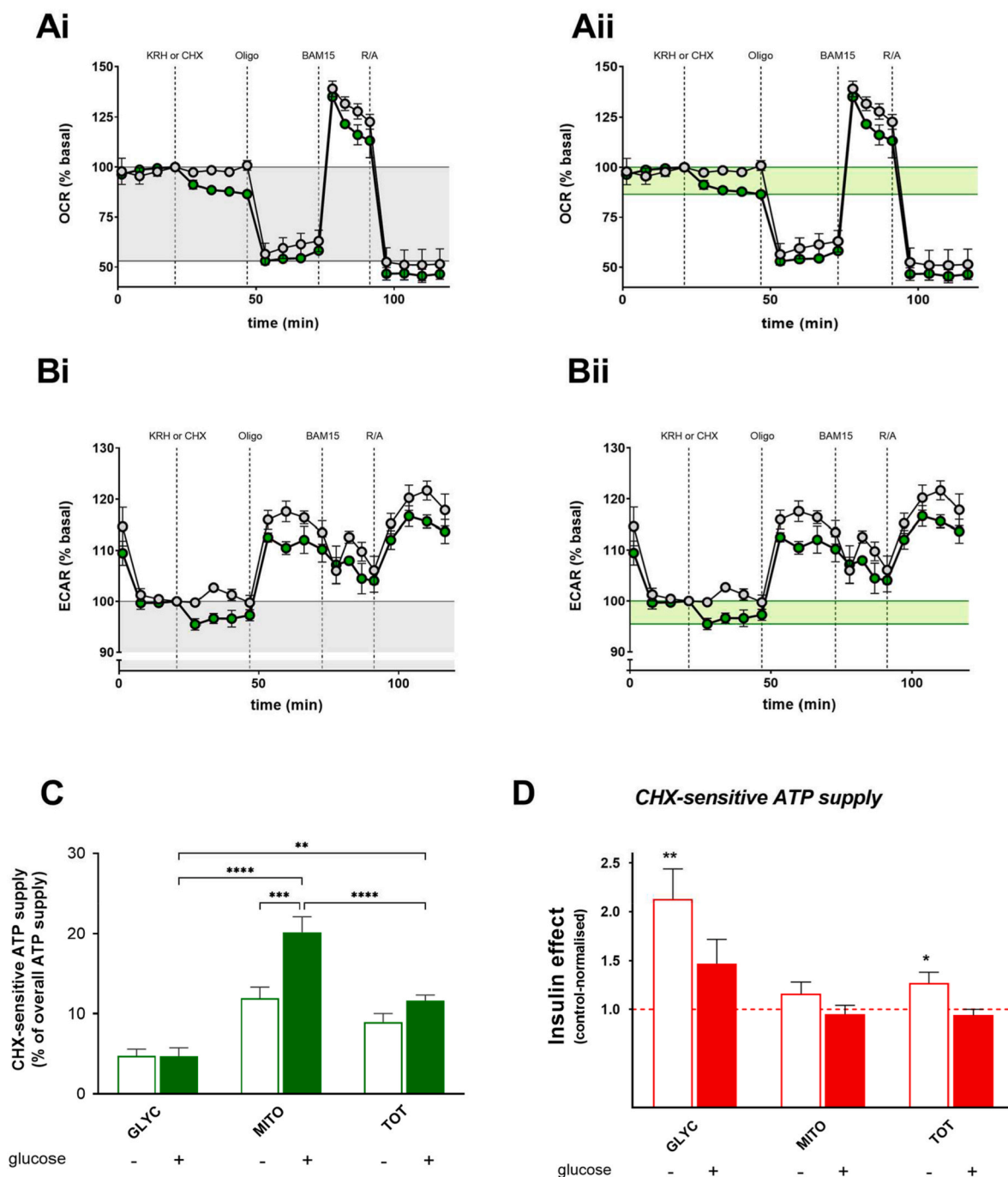
Fig. 3. – Effect of insulin on ATP demand in primary human myotubes. ATP demand from protein synthesis was estimated indirectly from XF data [23]. As shown by typical (means ± SEM of 3–5 measurements from a single experiment) OCR and ECAR traces (panels A and B), 1 μM cyclohexamide (CHX, green) or KRH (grey), 1.9 μg/mL oligomycin (Oligo), 1.5 μM BAM15, and 1 μM rotenone with 1 μM antimycin A (R/A) were added sequentially after 4 basal measurements. The oligomycin-sensitive OCR and basal ECAR in CHX traces (grey-shaded, panels Ai and Bi) were used to derive overall ATP supply, while the CHX-sensitive OCR and ECAR of the same traces were used to determine ATP supply used specifically to make protein (green-shaded, panels Aii and Bii). KRH traces were used to correct the CHX sensitivity for minor buffer addition effects. CHX-sensitive glycolytic (GLYC), mitochondrial (MITO) and total (TOT) ATP supply rates in untreated cells (expressed as percentage of the respective overall rates, panel C) and acute effects of 100 nM human insulin on these CHX-sensitive rates (panel D) were measured with and without 5 mM glucose. The insulin effects shown in panel D are expressed relative to the respective control parameters measured in the absence of insulin. Differences between CHX-sensitive ATP supply rates were tested for statistical significance by two-way ANOVA with Tukey's post-hoc analysis, while control-normalised insulin effects were tested for significance by one sample t tests (*P < 0.05, **P < 0.01, ****P < 0.0001). Data in panels C and D are means ± SEM of 4–21 and 13-23 separate measurements from 1 to 4 and 4 independent assays, respectively. (For interpretation of the references to colour in this figure legend, the reader is referred to the Web version of this article.)

and Krebs cycle are uncoupled from ATP synthesis and are no longer controlled by ATP demand. The difference in respiratory capacity (Fig. 1C) explains why substrate-level phosphorylation is higher in L6 myotubes than myoblasts (Fig. 1G). Myoblasts and myotubes increase glycolytic ATP supply to compensate for inhibited oxidative phosphorylation (Fig. 1G). However, the compensation is incomplete, as total ATP supply is somewhat lower under uncoupled than under basal conditions (Fig. 1G). The lack of full compensation indicates that glycolytic ATP supply has reached capacity.

3.2. Insulin stimulates glycolytic ATP supply

In line with our previous work [21], insulin acutely increases coupling efficiency of oxidative phosphorylation in L6 myocytes (Fig. 2A). In myoblasts, enhanced coupling is only apparent when cells were cultured in medium with 2% instead of 10% FBS from 16 h before the experiment, and were assayed without glucose, as we did before [21]. Interestingly, insulin more than doubles the rate at which myoblasts acidify the assay medium (Fig. 2B). Such acute stimulation is also seen in L6 myotubes, but the rate increase is less substantial (1.3-fold) and not statistically significant (Fig. 2B). This ECAR stimulation reflects elevated glycolytic ATP supply, the rate of which is increased 2.5- and 1.5-fold by insulin in L6 myoblasts (Fig. 2C) and myotubes (Fig. 2D), respectively. The glycolytic ATP supply rise is not at the expense of mitochondrial ATP synthesis, and insulin thus causes modest, but significant, increases in total cellular ATP supply (Fig. 2C and D). Consistent with stimulation of glycolytic ATP supply, insulin acutely raises the rate by which L6 myoblasts release lactate from 3.8 ± 0.39 to 5.1 ± 0.24 pmol/min/µg protein (Fig. 2E). Glycolytic ATP supply stimulation occurs regardless of glucose availability (Fig. 2C and D) and is thus unlikely secondary to a glucose uptake effect. Stimulation is still detectable under uncoupled conditions in myotubes (Fig. 2D), but not in myoblasts (Fig. 2C). Insulin also stimulates glycolytic ATP supply in human myotubes (Fig. 2F), which, similar to L6 cells, occurs without effect on mitochondrial ATP synthesis and thus raises total cellular ATP supply. Neither glycolytic nor total ATP supply is stimulated significantly in the absence of glucose. Under these conditions, insulin increases mitochondrial ATP supply (Fig. 2F). Glycolytic stimulation is lowered slightly under uncoupled conditions, but remains statistically significant (Fig. 2F).

3.3. Insulin increases glycolytic ATP supply used for protein synthesis

In L6 myoblasts, insulin stimulation of glycolytic ATP supply is abolished under uncoupled conditions (Fig. 2C), which indicates the effect is due to changes in ATP demand. Similarly, stimulation is attenuated under uncoupled conditions in human myotubes (Fig. 2F), which suggests that increased ATP demand may be partly responsible. To explore this possibility, we applied XF analysis [23] to test how insulin affects ATP demand from protein synthesis, a process that accounts for a significant proportion of mitochondrial ATP supply [28]. Inhibiting protein synthesis with cycloheximide lowers OCR (Fig. 3A) and ECAR (Fig. 3B), reflecting immediate adjustment of ATP supply to decreased energy expenditure [28]. The relatively small adjustment suggests that protein synthesis activity is fairly low in glucose-deprived human myotubes, with 5, 12 and 9% of glycolytic, mitochondrial and total ATP supply used for this process, respectively (Fig. 3C). In the presence of glucose, the respective proportions are about 5, 20 and 12%. As shown by the increased cycloheximide-sensitivity of total ATP supply (Fig. 3D), insulin stimulates protein synthesis, as is expected [29], but only in glucose-deprived cells. Notably, the ATP supply that permits this insulin stimulation is almost entirely glycolytic. These data show that the increase in glycolytic ATP supply in human myotubes partly follows from insulin-provoked ATP demand, which is consistent with the observation that stimulation is lower under uncoupled than under basal conditions (Fig. 2F).

3.4. Synergistic stimulation of glucose uptake by insulin and nitrite

In L6 myocytes, insulin stimulates glycolytic ATP supply regardless of extracellular glucose availability (Fig. 2C and D). Stimulation even tends to be amplified a little in myoblasts when assayed without glucose (Fig. 2C), which indicates the effect is not linked to glucose uptake. Confirming this, L6 myoblasts cultured with 2% instead of 10% FBS from 16 h before the experiment and assayed with 5 mM glucose (conditions we applied for measuring glucose uptake) make ATP by glycolysis in an insulin-sensitive way (Fig. 4A), but accumulate 2DG independently of insulin (Fig. 4B). Since nitrite has been reported to increase recruitment of insulin-sensitive glucose transporters [30], we also tested the acute effect of 1 µM NaNO$_2$ on (insulin-sensitive) ATP supply and 2DG uptake. Similar to insulin, nitrite increases glycolytic ATP supply (Fig. 4A) without affecting 2DG accumulation (Fig. 4B). Sequential exposure to nitrite and insulin does not stimulate glycolytic ATP supply more strongly than individual exposure (Fig. 4A). Such combined exposure almost doubles 2DG accumulation (Fig. 4B), which indicates that nitrite and insulin increase glucose uptake in a synergistic manner. The difference in nitrite-insulin interaction further supports our assertion that insulin-sensitivity of glycolytic ATP supply is unrelated to glucose uptake. Nitrite thus increases insulin sensitivity of glucose uptake, but not of ATP supply.

3.5. Multifarious insulin stimulation of glycolytic ATP supply

The results shown above highlight how simultaneous measurement of oxygen consumption and medium acidification by cultured cells offers much insight in cellular energy metabolism when such measurements are used to quantify ATP flux. We thus show that insulin stimulates glycolytic ATP supply in skeletal muscle cells. This stimulation is acute and achieved directly by effects on glycolytic capacity, and indirectly by elevation of ATP demand from protein synthesis.

ATP flux in well-nourished healthy skeletal muscle is largely controlled by ATP demand [16]. Such control allows cells to keep their phosphorylation potential constant, and far removed from equilibrium, under a wide range of energy demands. Conditions of high energy demand may be mimicked experimentally by exposing cells to uncouplers (BAM15) that dissipate the cell's phosphorylation potential [31]. Uncoupled cells increase glycolysis to compensate for inhibited oxidative phosphorylation (Fig. 1G). Incomplete compensation shows ATP demand cannot be met by glycolysis alone, which must thus be running at capacity.

In L6 (Fig. 2D) and human (Fig. 2F) myotubes, insulin raises glycolytic ATP supply under both basal and uncoupled conditions and thus boosts glycolytic *capacity*. This observation agrees with the reported insulin stimulation of the activity of glycolytic enzymes, notably hexokinase and phosphofructokinase [32]. Stimulation of hexokinase includes transcriptional and translational upregulation of protein expression as well as activation of existing enzyme [33], which would be consistent with the immediate nature of insulin stimulation of glycolytic ATP supply. However, stimulation is also evident in nutrient-deprived L6 myocytes (Fig. 2C and D) that fuel energy metabolism with glycogen, i.e., independently of hexokinase. Related, enhanced glucose uptake is not responsible for boosted glycolytic capacity, because insulin stimulates ATP supply regardless of glucose availability (Fig. 2C and D), and because nitrite amplifies insulin sensitivity of glucose uptake (Fig. 4B) without effect on bioenergetic insulin sensitivity (Fig. 4A).

Insulin stimulation of glycolytic ATP supply is lowered somewhat by uncoupling in human myotubes (Fig. 2F) and completely abolished in L6 myoblasts (Fig. 2C), which implies that elevated ATP demand indirectly contributes to the stimulation. Increased ATP demand is caused by insulin-induced protein synthesis (Fig. 3D), but insulin activates other anabolic processes that may all increase energy expenditure in principle [16]. Inversely, dampened stimulation of anabolism in insulin-resistant muscle will lower energy demand and thus ATP synthesis. For instance,
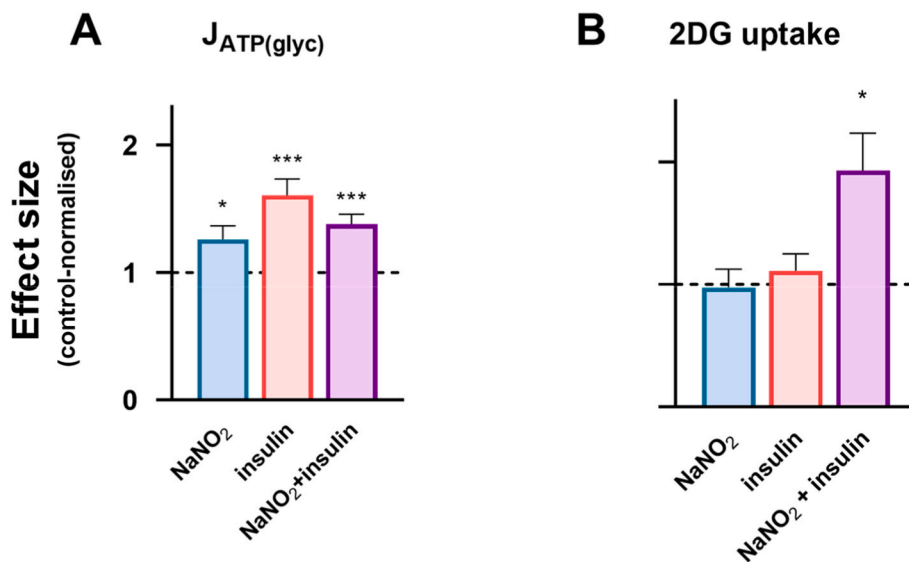
Fig. 4. – Insulin stimulation of glycolytic ATP supply is not linked to glucose uptake. Glycolytic ATP supply (panel A – $J_{ATP(glyc)}$) was measured in L6 myoblasts under conditions identical to those applied for the 2DG (2-deoxyglucose) uptake assay (panel B), i.e., cells were cultured at 2% FBS from 16 h before the experiment and 5 mM glucose was added during the XF assay before other effectors. Cells were exposed transiently to 1 μM NaNO$_2$ for 20 min before the assay and both exposed and non-exposed cells were assayed with or without 100 nM human insulin. Effects are means ± SEM of 12–15 separate measurements from 3 to 4 independent experimental runs and were normalised to the values obtained in cells exposed to neither nitrite nor insulin. Effects were evaluated for statistical significance by one sample t tests (*P < 0.05, ***P < 0.001).

palmitate reallocates mitochondrial ATP supply to ATP-consuming processes while causing insulin-resistance of glucose uptake by cultured muscle cells [28].

Together, our data reveal that insulin stimulates glycolytic ATP supply via multiple targets. We assert that the relative importance of these targets depends on the control distribution between ATP supply and ATP demand. The extent to which overall ATP flux is controlled by (glycolytic and mitochondrial) ATP supply and ATP demand is fluid and depends on many factors including nutrient availability and muscle health. Our findings underscore the risk of interpreting ATP supply changes without paying attention to energy expenditure. Notably, in this respect, depressed oxidative phosphorylation is often taken as support for mitochondrial dysfunction without considering the possibility that it just reflects adaptation to altered ATP demand. For instance, apparent discrepancies on the causal relation between mitochondrial ATP synthesis and muscle insulin resistance are readily reconciled when energy metabolism is considered holistically [16].

In conclusion, the results reported in this paper highlight the multifactorial nature of the bioenergetic insulin sensitivity of skeletal muscle cells. The direct demonstration that ATP supply adjusts acutely to insulin-provoked changes in energy demand is important for interpreting the bioenergetic 'failure' that is observed in insulin-resistant muscle.

Funding

Author contributions

RAD and JEC designed and performed experiments, analysed and interpreted data, and edited and approved the manuscript. CA conceived the study, performed experiments, analysed and interpreted data, and wrote the manuscript.

Declaration of competing interest

The authors declare no conflict of interest. The sponsors (Daphne Jackson Trust, Kidney Research UK and the University of Plymouth) had no role in the design, execution, interpretation or writing of the study. It was the decision of the authors only to submit the manuscript for publication.

Acknowledgements

References

[1] D. Thiebaud, E. Jacot, R.A. DeFronzo, E. Maeder, E. Jequier, J.P. Felber, The effect of graded doses of insulin on total glucose uptake, glucose oxidation, and glucose storage in man, Diabetes 31 (1982) 957–963.

[2] R.A. DeFronzo, From the triumvirate to the ominous octet: a new paradigm for the treatment of type 2 diabetes mellitus, Diabetes 58 (2009) 773–795.

[3] G.A. Rutter, T.J. Pullen, D.J. Hodson, A. Martinez-Sanchez, Pancreatic β-cell identity, glucose sensing and the control of insulin secretion, Biochem. J. 466 (2015) 203–218.

[4] A.J. Garber, Obesity and type 2 diabetes: which patients are at risk? Diabetes Obes. Metabol. 14 (2012) 399–408.

[5] M.C. Petersen, G.I. Shulman, Mechanisms of insulin action and insulin resistance, Physiol. Rev. 98 (2018) 2133–2223.

[6] M. Lytrivi, A.-L. Castell, V. Poitout, M. Cnop, Recent insights into mechanisms of beta-cell lipo- and glucolipotoxicity in type 2 diabetes, J. Mol. Biol. 432 (2020) 1514–1534.

[7] A. Armandi, C. Rosso, G.P. Caviglia, D.G. Ribaldone, E. Bugianesi, The impact of dysmetabolic sarcopenia among insulin sensitive tissues: a narrative review, Front. Endocrinol. 12 (2021), 716533.

[8] T. Dao, A.E. Green, Y.A. Kim, S.-J. Bae, K.-T. Ha, K. Gariani, M.-R. Lee, K. J. Menzies, D. Ryu, Sarcopenia and muscle aging: a brief overview, Endocrinol. Metab. 35 (2020) 716–732.

[9] S. Dasarathy, M. Merli, Sarcopenia from mechanism to diagnosis and treatment in liver disease, J. Hepatol. 65 (2016) 1232–1244.

[10] I.H. Fahal, Uraemic sarcopenia: aetiology and implications, Nephrol. Dial. Transplant. 29 (2014) 1655–1665.

[11] J.O. Holloszy, Exercise-induced increase in muscle insulin sensitivity, J. Appl. Physiol. 99 (2005) 338–343.

[12] D.G. Hardie, AMPK - sensing energy while talking to other signaling pathways, Cell Metabol. 20 (2014) 939–952.

[13] G.K. McConell, B.A. Kingwell, Does nitric oxide regulate skeletal muscle glucose uptake during exercise? Exerc. Sport Sci. Rev. 34 (2006) 36–41.

[14] S. Moncada, A. Higgs, The L-arginine-nitric oxide pathway, N. Engl. J. Med. 329 (1993) 2002–2012.

[15] J.O. Lundberg, M. Carlström, E. Weitzberg, Metabolic effects of dietary nitrate in health and disease, Cell Metabol. 28 (2018) 9–22.

[16] C. Affourtit, Mitochondrial involvement in skeletal muscle insulin resistance: a case of imbalanced bioenergetics, Biochim. Biophys. Acta 1857 (2016) 1678–1693.

[17] T. Tiganis, Reactive oxygen species and insulin resistance: the good, the bad and the ugly, Trends Pharmacol. Sci. 32 (2011) 82–89.

[18] C.S. Stump, K.R. Short, M.L. Bigelow, J.M. Schimke, K.S. Nair, Effect of insulin on human skeletal muscle mitochondrial ATP production, protein synthesis, and mRNA transcripts, Proc. Natl. Acad. Sci. Unit. States Am. 100 (2003) 7996–8001.

[19] K.F. Petersen, S. Dufour, G.I. Shulman, Decreased insulin-stimulated ATP synthesis and phosphate transport in muscle of insulin-resistant offspring of type 2 diabetic parents, PLoS Med. 2 (2005) e233.

[20] A. Brehm, M. Krssak, A.I. Schmid, P. Nowotny, W. Waldhäusl, M. Roden, Increased lipid availability impairs insulin-stimulated ATP synthesis in human skeletal muscle, Diabetes 55 (2006) 136–140.

[21] R.B. Nisr, C. Affourtit, Insulin acutely improves mitochondrial function of rat and human skeletal muscle by increasing coupling efficiency of oxidative phosphorylation, Biochim. Biophys. Acta 1837 (2014) 270–276.

[22] H.S. Brunetta, H.L. Petrick, B. Vachon, E.A. Nunes, G.P. Holloway, Insulin rapidly increases skeletal muscle mitochondrial ADP sensitivity in the absence of a high lipid environment, Biochem. J. 478 (2021) 2539–2553.

[23] S.A. Mookerjee, A.A. Gerencser, D.G. Nicholls, M.D. Brand, Quantifying intracellular rates of glycolytic and oxidative ATP production and consumption using extracellular flux measurements, J. Biol. Chem. 292 (2017) 7189–7207.

[24] A.A. Gerencser, A. Neilson, S.W. Choi, U. Edman, N. Yadava, R.J. Oh, D.A. Ferrick, D.G. Nicholls, M.D. Brand, Quantitative microplate-based respirometry with correction for oxygen diffusion, Anal. Chem. 81 (2009) 6868–6878.

[25] P.K. Smith, R.I. Krohn, G.T. Hermanson, A.K. Mallia, F.H. Gartner, M. D. Provenzano, E.K. Fujimoto, N.M. Goeke, B.J. Olson, D.C. Klenk, Measurement of protein using bicinchoninic acid, Anal. Biochem. 150 (1985) 76–85.

[26] S.A. Mookerjee, M.D. Brand, Measurement and analysis of extracellular acid production to determine glycolytic rate, J. Vis. Exp. 106 (2015), e53464.

[27] M.D. Brand, D.G. Nicholls, Assessing mitochondrial dysfunction in cells, Biochem. J. 435 (2011) 297–312.

[28] R.B. Nisr, C. Affourtit, Palmitate-induced changes in energy demand cause reallocation of ATP supply in rat and human skeletal muscle cells, Biochim. Biophys. Acta 1857 (2016) 1403–1411.

[29] C.G. Proud, Regulation of protein synthesis by insulin, Biochem. Soc. Trans. 34 (2006) 213–216.

[30] H. Jiang, A.C. Torregrossa, A. Potts, D. Pierini, M. Aranke, H.K. Garg, N.S. Bryan, Dietary nitrite improves insulin signaling through GLUT4 translocation, Free Radic. Biol. Med. 67 (2014) 51–57.

[31] C. Affourtit, B. Alberts, J. Barlow, J.E. Carré, A.G. Wynne, Control of pancreatic β-cell bioenergetics, Biochem. Soc. Trans. 46 (2018) 555–564.

[32] G. Dimitriadis, P. Mitron, V. Lambadiari, E. Maratou, S.A. Raptis, Insulin effects in muscle and adipose tissue, Diabetes Res. Clin. Pract. 93 (2011) S52–S59.

[33] L.J. Mandarino, R.L. Printz, K.A. Cusi, P. Kinchington, R.M. O'Doherty, H. Osawa, C. Sewell, A. Consoli, D.K. Granner, R.A. DeFronzo, Regulation of hexokinase II and glycogen synthase mRNA, protein, and activity in human muscle, Am. J. Physiol. 269 (1995) E701–E708.